AMERICAN SOCIETY FOR MICROBIOLOGY | Antimicrobial Agents and Chemotherapy

Stearylamine Liposomal Delivery of Monensin in Combination with Free Artemisinin Eliminates Blood Stages of *Plasmodium falciparum* in Culture and *P. berghei* Infection in Murine Malaria

Vinoth Rajendran,[a] Shilpa Rohra,[a] Mohsin Raza,[a] Gulam Mustafa Hasan,[a]* Suparna Dutt,[b] Prahlad C. Ghosh[a]

Department of Biochemistry, University of Delhi South Campus, New Delhi, India[a]; Department of Medicine, Division of Immunology and Rheumatology, Stanford University School of Medicine, Stanford, California, USA[b]

The global emergence of drug resistance in malaria is impeding the therapeutic efficacy of existing antimalarial drugs. Therefore, there is a critical need to develop an efficient drug delivery system to circumvent drug resistance. The anticoccidial drug monensin, a carboxylic ionophore, has been shown to have antimalarial properties. Here, we developed a liposome-based drug delivery of monensin and evaluated its antimalarial activity in lipid formulations of soya phosphatidylcholine (SPC) cholesterol (Chol) containing either stearylamine (SA) or phosphatidic acid (PA) and different densities of distearoyl phosphatidylethanolamine-methoxy-polyethylene glycol 2000 (DSPE-mPEG-2000). These formulations were found to be more effective than a comparable dose of free monensin in *Plasmodium falciparum* (3D7) cultures and established mice models of *Plasmodium berghei* strains NK65 and ANKA. Parasite killing was determined by a radiolabeled [^{3}H]hypoxanthine incorporation assay (*in vitro*) and microscopic counting of Giemsa-stained infected erythrocytes (*in vivo*). The enhancement of antimalarial activity was dependent on the liposomal lipid composition and preferential uptake by infected red blood cells (RBCs). The antiplasmodial activity of monensin in SA liposome (50% inhibitory concentration [IC_{50}], 0.74 nM) and SPC:Chol-liposome with 5 mol% DSPE-mPEG 2000 (IC_{50}, 0.39 nM) was superior to that of free monensin (IC_{50}, 3.17 nM), without causing hemolysis of erythrocytes. Liposomes exhibited a spherical shape, with sizes ranging from 90 to 120 nm, as measured by dynamic light scattering and high-resolution electron microscopy. Monensin in long-circulating liposomes of stearylamine with 5 mol% DSPE-mPEG 2000 in combination with free artemisinin resulted in enhanced killing of parasites, prevented parasite recrudescence, and improved survival. This is the first report to demonstrate that monensin in PEGylated stearylamine (SA) liposome has therapeutic potential against malaria infections.

Malaria is caused by the protozoan parasite *Plasmodium*, transmitted through the bites of infected female *Anopheles* mosquitoes to humans. Of all the species in its genus, *Plasmodium falciparum* is the most virulent and lethal human malarial pathogen that causes cerebral malaria. Unfortunately, it is developing varied degrees of resistance to available antimalarial drugs (1). Currently, artemisinin-based monotherapies show early clinical resistance toward *P. falciparum* in various parts of Southeast Asian countries, mostly on the Cambodia-Thailand border (2, 3). Clinical resistance is attributed to the slow clearance of parasites in response to artemisinin-based therapies (4–7). In particular, individuals coinfected with HIV and *P. falciparum* and *Plasmodium vivax* strains are unresponsive to this treatment (8). The development of clinical drug resistance in malarial parasites poses a major obstacle in conventional chemotherapy (9). Importantly, the overuse of chloroquine (CQ) for *Plasmodium* infection treatment leads to quinolone resistance in commensal *Escherichia coli* strains in humans (10). To obviate drug resistance, efforts are being made to develop artemisinin-based combination therapies (ACTs), develop new drugs, and improve the efficiency of drug delivery vehicles of existing antimalarial drugs.

Monensin, a polyether antibiotic ionophore, has been shown to exhibit antimalarial activity against *P. falciparum in vitro* (11, 12) and *Plasmodium vinckei petteri* and *Plasmodium chabaudi in vivo* (12, 13). This ionophore carries Na^+ across intracellular organelle membranes and facilitates the exchange of H^+. This results in elevated Na^+ concentrations in parasite vacuoles, with an increase in intralysosomal pH and lysosomal protein degradation (14). It also exhibits divergent activities, such as antitumor effects (15, 16) and potentiation of immunotoxins (17, 18), and it is an antibacterial (19) and anticoccidial agent for the treatment of avian coccidiosis (20). However, due to the strong hydrophobic and lipophilic nature of monensin, it was either administered in ethanolic solution, in a dimethyl sulfoxide (DMSO) solution, conjugated with serum albumin (21), or emulsified in gum Arabic and Tween 80 (12). These agents, however, are inappropriate for clinical use.

Liposomes have been used as potential delivery vehicles for hydrophobic drugs (22, 23). Drug delivery systems based on liposomes have been shown to protect drugs, increase their therapeutic index, prolong their systematic circulation time, lower intrinsic

Received 11 August 2015 **Returned for modification** 27 August 2015
Accepted 4 December 2015

Accepted manuscript posted online 14 December 2015

Citation Rajendran V, Rohra S, Raza M, Hasan GM, Dutt S, Ghosh PC. 2016. Stearylamine liposomal delivery of monensin in combination with free artemisinin eliminates blood stages of *Plasmodium falciparum* in culture and *P. berghei* infection in murine malaria. Antimicrob Agents Chemother 60:1304–1318. doi:10.1128/AAC.01796-15.

Address correspondence to Prahlad C. Ghosh, pcghose@gmail.com, or Vinoth Rajendran, vinoth.avj@gmail.com.

* Present address: Gulam Mustafa Hasan, Department of Biochemistry, College of Medicine, Prince Sattam Bin Abdulaziz University, Al-Kharj, Saudi Arabia.

toxicity, and reduce immunogenicity (24, 25). We have developed liposomal formulations of monensin that were shown to potentiate the toxicity of ricin in animal models (26). In malaria, merozoite surface protein 1 (MSP-1) entrapped in liposomes has been used as a vaccine (27). Liposomes containing glycolipids with terminal galactose or glucose on the surface when injected into *Plasmodium berghei* sporozoite-infected mice prevented the appearance of asexual stages and hepatic infection (28). To overcome mild drug resistance, liposomes were used to deliver chloroquine for the treatment of CQ-resistant malaria (29). Liposomes bearing infected erythrocyte-specific antibodies have been used for the targeted delivery of chloroquine (30). However, no lipid-based nanoformulations for hydrophobic antimalarials have been reported. Based on these studies, we hypothesized that liposomes could serve as an efficient and safe delivery vehicle for hydrophobic antimalarial drugs. However, the relatively short half-life of these liposomes is a major challenge for use *in vivo*. Therefore, we tested the antimalarial activity of monensin in long-circulating sterically stabilized liposomes (SSL) with distearoyl phosphatidylethanolamine-methoxy-polyethylene glycol 2000 (DSPE-mPEG 2000). The present investigation focuses on the development of an effective liposomal delivery for monensin and an evaluation of antimalarial activity on various blood stages of *P. falciparum* (3D7) *in vitro*, in murine malaria induced by *P. berghei* NK65 and lethal strain *P. berghei* ANKA, and in combination therapy with free artemisinin. This study demonstrates our proof of concept of using liposome-mediated delivery of hydrophobic antimalarial drugs.

MATERIALS AND METHODS

Materials. Soya phosphatidylcholine (SPC) was obtained as a gift from Lifecare Innovations Pvt. Ltd., Haryana, India. Monensin sodium salt (MON), cholesterol (Chol), stearylamine (SA), artemisinin (ART), chloroquine diphosphate (CQ), coumarin-6, calcein, DAPI (4′,6-diamidino-2-phenylindole), gentamicin sulfate (cell culture grade), and Histopaque-1077 were purchased from Sigma-Aldrich (St. Louis, MO, USA). L-α-Phosphatidic acid (PA), DSPE-mPEG 2000, and NBD-PC (1-palmitoyl-2-sn-glycero-3-phosphocholine) were purchased from Avanti Polar Lipids, Inc., AL, USA. Powdered RPMI 1640 medium, AlbuMAX II, and octadecyl rhodamine B (R18) are Gibco products from the Invitrogen Corporation. Hypoxanthine monohydrochloride ([^{3}H(G)]) was bought from American Radiolabeled Chemicals, Inc., St. Louis, MO, USA. All other chemicals were analytical-grade products.

Animals. All animal experiments were performed in female Swiss albino mice (4 to 5 weeks old, weighing 25 to 30 g). These mice were obtained from the laboratory of Lala Lajpat Rai University of Veterinary and Animal Sciences, India, and maintained in our animal facility at the University of Delhi South Campus, New Delhi, India. The animals were housed under standard controlled conditions at 25°C with a 12-h light-dark cycle and access to sterilized food pellets and water. All experiments were carried out in accordance with the standard procedures approved by the Animal Ethics Committee of the University of Delhi South Campus, under the Control and Supervision of Experiments on Animals (CPCSEA), Ministry of Social Justice and Empowerment, Government of India.

Preparation of liposomes. Liposomes were prepared using soya phosphatidyl choline (SPC) and cholesterol (Chol) in a molar ratio of 7:3 by manual shaking. Briefly, the lipids (total, 200 μmol) and monensin (10 mol% of the lipid mixture) were dissolved in a chloroform solution. To prepare other formulations, 10 mol% either phosphatidic acid (PA) or stearylamine (SA) was added during the preparation of lipid film. The dried lipid film so obtained was desiccated overnight and then was hydrated with 20 mM sterile phosphate-buffered saline (PBS), stored under a nitrogen atmosphere, and sonicated. For the preparation of sterically stabilized liposomes (SSL) with different molar percentages of DSPE-mPEG 2000 (0.5, 2.5, and 5 mol%), which was added during the preparation of lipid film. For fluorescent labeling of the liposomes, NBD-PC–coumarin-6–octadecylrhodamine B (R18) was dissolved, along with lipids containing 1 mol% in each formulation and 80 mM calcein added to the lipid suspension. Liposomal monensin was separated from the unentrapped monensin, undispersed lipids, and calcein by centrifugation at 1,956 × *g* and 4°C for 15 min and further subjected to ultracentrifugation at 11,800 × *g* for 1 h. The liposomal suspension was assayed colorimetrically for the presence of monensin, according to the method described in reference 31. The recovery of liposomes was determined colorimetrically by measuring phospholipids using Stewart's method (32).

Determination of size distribution and zeta potential of liposomal monensin using dynamic laser light scattering. The liposome size (in nanometers) and zeta potential (ζ) were measured using a Zetasizer Nano ZS (ZEN 3600; Malvern Instruments, Worcestershire, United Kingdom). For the measurements, 10 μl of sample suspension was dispersed in 990 μl of PBS and sonicated for 1 min. The parameters set for analyses were a scattering angle of 90° and a temperature of 25°C. For each sample, the mean diameter and the standard deviation of 10 determinations were calculated using multimodal analysis. The zeta potential was measured by a combination of laser Doppler velocimetry and phase analysis light scattering (M3-PALS) technique at 25°C.

Transmission electron microscopy of various liposomal formulations containing monensin. The sample preparation was performed by taking 10 μl of diluted liposomal suspension placed upon 300-mesh carbon-coated copper grids under sterile conditions and air drying for analysis (Polysciences, Warrington, PA). The liposomes were visualized under a Tecnai G2 T30 U-TWIN electron microscope, and images were obtained using a digital imaging software at different magnifications.

***In vitro* culture of *P. falciparum*.** The strain of *P. falciparum* used in the study was 3D7, obtained from Suman Dhar's laboratory at the Special Centre for Molecular Medicine (Jawaharlal Nehru University, New Delhi, India). The whole O+ blood was obtained from the Rotary Blood Bank, New Delhi, India. This strain was maintained by serial passages in human erythrocytes cultured at 4 to 5% hematocrit in RPMI 1640 medium supplemented with 0.5% AlbuMAX II and gentamicin sulfate (here referred to as complete RPMI 1640) and incubated at 37°C under an atmosphere of mixed gas (5% CO_2, 5% O_2, and 90% N_2). The red blood cells (RBCs) were obtained under sterile conditions by the removal of plasma and peripheral blood mononuclear cells (PBMCs) using a Histopaque gradient; the RBCs were washed 2 to 3 times using RPMI 1640 without AlbuMAX II (incomplete media).

Evaluation of antimalarial activity of monensin in various liposomal formulations *in vitro*. The effect of monensin in various liposomal formulations *in vitro* was evaluated by checking its ability to inhibit the incorporation of a radiolabeled precursor, [^{3}H]hypoxanthine, in the nucleic acids of parasites. In brief, asynchronous *P. falciparum* cultures were maintained in complete RPMI 1640 and plated on 96-well microdilution plates (4% final hematocrit and 2% parasitemia) in a total volume of 200 μl and incubated with different concentrations of liposomal monensin in RPMI 1640. The synchronization of erythrocytic stages in culture was carried out using 5% sorbitol (52). After 24 h of incubation at 37°C, 20 μl of 0.2 μCi/well [^{3}H]hypoxanthine was added to each well for an additional 18 h. At the end of incubation, the contents in each well were harvested on a glass-fiber filter mat using a 96-well Skatron semiautomated cell harvester. The [^{3}H]hypoxanthine uptake, an index of cell viability, was measured by transferring the paper disc to a scintillation vial containing 5 ml of a toluene-based scintillation cocktail and counted in a PerkinElmer liquid scintillation analyzer β-counter (TriCarb 2900TR). The 50% inhibitory concentrations (IC_{50}s) were determined from parasite-associated radioactivity by plotting the drug concentration versus the percentage of cell viability of the parasite after 42 h of a growth assay period. All data points were collected in triplicate for each experiment. The drug interaction studies were calculated using the formula for the

50% fractional inhibitory concentration (FIC_{50}) values of each drug: IC_{50} for drug in combination/IC_{50} for drug alone.

Development of murine model of rodent strains. For the experimental infections, a murine model of malaria was developed by intraperitoneal (i.p.) injection of 10^5 to 10^7 rodent-specific *P. berghei* NK65-infected (noncerebral)- and *P. berghei* ANKA-infected (cerebral malaria) erythrocytes to healthy Swiss albino mice weighing 25 to 30 g. Parasitemia was monitored routinely by continuous weekly blood passages of parasitized erythrocytes (PE) from infected to naive mice, and survival was checked over a period of 2 weeks.

***In vivo* antimalarial study.** To examine the therapeutic efficacy of various liposomal formulations of monensin, a murine model of malaria was developed by i.p. administration of standard inoculum of two rodent strains of *P. berghei* NK65 and *P. berghei* ANKA carrying 1×10^7 parasitized erythrocytes per 200 μl volume to each experimental Swiss albino mouse. The *in vivo* antimalarial activity of monensin in various liposomal formulations was carried out in accordance with a slightly modified version of the Peter's 4-day suppressive test (33). The animals were assigned to each group. Subsequently, after 48 h of postinfection, the parasitemia level reached 1 to 2%, and all groups of mice were treated by subcutaneous (s.c.) injection with free and liposomal monensin in a dose-dependent manner with 2, 4, 6, or 8 mg/kg of body weight and free artemisinin (ART) at 10, 20, or 40 mg/kg of body weight given in a combination treatment. One group was kept as a control and treated with physiological saline. The efficacy of the treatment was monitored by measuring the parasitemia and survival on days 5, 8 and 15 posttreatment by obtaining thin smears of blood drawn from the tail vein of infected mice and staining with 10% Giemsa. The level of parasitemia was determined by counting infected and noninfected erythrocytes from 10 to 15 randomly selected optical fields at 100× magnification and expressed as the number of infected erythrocytes per 100 erythrocytes. The survival of mice was recorded and observed for external symptoms, such as change in body weight, ruffled fur, lethargy, and paralysis, until 30 or 40 days posttreatment. The reduction in the level of parasitemia was taken as the index for the curative activities of the drugs. The percentage of parasitemia was calculated manually with the Cell Counting Aid software (34), using the formula (total no. of parasitized RBCs)/(total no. of RBCs) × 100.

Histopathological evaluation. For histopathological examination, representative samples of liver tissue were excised from *P. berghei* NK65-infected mice on day 15 postinfection, which had 40 to 50% parasitemia in the untreated group. The treated group was administered four doses of 8 mg/kg of body weight of free monensin and various liposomal formulations containing monensin, as described earlier; liver tissue was collected aseptically. The tissue samples were fixed in 10% neutral-buffered formalin for analysis. Further, formalin-fixed and paraffin-embedded tissues were used to prepare 5-μm-thick sections, and these were stained with hematoxylin and eosin (H&E). The tissue samples were coded and analyzed by a certified pathologist with no knowledge of the experimental groups. Tissue sections were evaluated by light microscopy, and the images were taken using the 400× objective of a Leica DM5000 microscope. The whole-liver section was examined to determine the presence of hemozoin pigment deposits and other morphological features.

Assessment of plasma clearance and biodistribution of monensin in various liposomal formulations labeled with a fluorescent surface marker (NBD-PC) in normal and infected mice. Biodistribution studies were performed in normal mice and mice infected with *P. berghei* NK65 on day 10 postinfection, as described earlier, using three animals in each group. All mice were administered subcutaneously a single dose of fluorescently labeled NBD-PC with various liposomal formulations containing monensin. Each group of mice was sacrificed at different time intervals (1, 4, 12, 24, and 48 h) after the injection of the liposomal formulations. Blood was drawn in tubes containing heparin (50 units/ml) to obtain plasma, and various organ tissues (liver, kidney, spleen, lungs, and brain) were excised and washed with saline. The obtained plasma and tissue samples were homogenized using chloroform-methanol (2:1), centrifuged at 7,826 × *g* for 30 min, and the supernatant was analyzed for the presence of NBD-PC by monitoring the fluorescence intensity in a spectrofluorimeter (Varian Cary Eclipse) at excitation and emission wavelengths of 460 and 534 nm, respectively. The uninjected liposomes from normal and infected animals were used as a control. The fluorescence values in the experimental mice were corrected for any endogenous fluorescence.

***In vitro* and *ex vivo* uptake of fluorescently tagged liposomal formulations by *P. falciparum* 3D7 in culture and *P. berghei* NK65-infected erythrocytes.** To detect the uptake of SA liposome and PEGylated liposomal monensin in both *P. falciparum*-infected erythrocytes and uninfected erythrocytes, the coumarin-6-labeled liposome fluorescent marker was used. In brief, *P. falciparum*-infected erythrocytes (10% hematocrit and 10% parasitemia) were incubated in the presence of liposomal formulations. The uptake in erythrocytes was assessed at different time intervals (15, 30, 60, 120, and 240 min) under asynchronous culture at 37°C. At the end of the incubation, the cells were washed twice with incomplete RPMI 1640 medium to remove unbound liposomes, and the obtained RBC pellet was resuspended in chloroform to extract intracellular fluorescence, which is released into the supernatant. The fluorescence intensity of coumarin-6 from the RBC extract was measured using a Varian Cary Eclipse spectrofluorimeter, with excitation and emission wavelengths set at 460 nm and 495 nm, respectively. To further investigate the uptake of liposomes by parasite-infected erythrocytes, liposomes were dually labeled with the fluorescent dye octadecylrhodamine (R18) as the lipid dye and calcein as an aqueous fluorophore. An *ex vivo* uptake study was conducted in heavily parasitized *P. berghei* NK65-infected mouse erythrocytes, which were stained with 1 μg/ml DAPI and incubated for 15 min at 37°C. The stained cells were visualized by fluorescence microscopy (Nikon Ellipse Ti-S) at 100× magnification.

Hemolytic assay. The toxicities of various liposomal formulations in normal and infected erythrocytes were assessed by measuring the lysis of RBCs in the culture medium. Different concentrations of free monensin and various formulations of liposomal monensin were added to normal RBCs at 4% hematocrit and infected RBCs at 4% hematocrit and 2% parasitemia, as reported earlier (35).

Statistical analysis. For the *in vitro* studies, the data are presented as the mean ± standard error of the results from at least three independent experiments. For the *in vivo* experiments, statistical differences between two groups were determined by Student's *t* test and between multiple groups using one-way analysis of variance (ANOVA), with *P* values of <0.05, by GraphPad Prism (version 5.01; GraphPad Software, Inc., CA). The survival of the mice was followed up to day 30 or 40 postinfection using Kaplan-Meier survival analysis, and statistical differences in animal survival were analyzed by a log rank test.

RESULTS

Determination of size and zeta potential of monensin in various liposomal formulations. The size (in nanometers) and surface charge (ζ potential) of various liposomal formulations were determined using dynamic laser light scattering (DLS) and suspended in phosphate-buffered saline, as shown in Table 1. The mean diameter ranging from 90 to 120 nm was obtained in all liposomal formulations. The change in surface zeta potential (ζ) values was dependent on the incorporation of charged lipids (SA and PA) and the different densities of DSPE-mPEG 2000. It was shown that an increase in PEG polymer (0.5 to 5 mol%) on the surface resulted in sharp decrease in ζ-potential values.

TEM studies of various liposomal formulations containing monensin. Transmission electron microscopy (TEM) is the most extensively used experimental technique, which provides two-dimensional images of nanosized particles. TEM enables one to obtain general information on particle morphology and precisely

TABLE 1 Determination of size and zeta potential of monensin in various liposomal formulations[a]

Liposome formulation	mol% of DSPE-mPEG 2000	Size (nm)	Zeta potential (ζ) (mV)	PDI[b]
SPC + Chol + MON (neutral)		124 ± 10	−11.6 ± 0.66	0.283 ± 0.006
SPC + Chol + MON + DSPE-mPEG 2000	0.5	103 ± 14	−14.5 ± 0.74	0.273 ± 0.009
SPC + Chol + MON + DSPE-mPEG 2000	2.5	96 ± 11	−12.6 ± 0.52	0.314 ± 0.010
SPC + Chol + MON + DSPE-mPEG 2000	5.0	90 ± 10	−8.8 ± 0.35	0.277 ± 0.004
SPC + Chol + MON + PA (negative)		109 ± 15	−23.3 ± 0.46	0.294 ± 0.011
SPC + Chol + MON + PA + DSPE-mPEG 2000	0.5	98 ± 18	−29.5 ± 0.87	0.233 ± 0.009
SPC + Chol + MON + PA + DSPE-mPEG 2000	2.5	100 ± 09	−18.4 ± 0.78	0.217 ± 0.010
SPC + Chol + MON + PA + DSPE-mPEG 2000	5.0	98 ± 11	−12.7 ± 0.82	0.216 ± 0.005
SPC + Chol + MON + SA (positive)		121 ± 20	43.9 ± 0.90	0.247 ± 0.012
SPC + Chol + MON + SA + DSPE-mPEG 2000	0.5	107 ± 18	34.7 ± 0.71	0.277 ± 0.008
SPC + Chol + MON + SA + DSPE-mPEG 2000	2.5	101 ± 14	18.9 ± 0.32	0.239 ± 0.011
SPC + Chol + MON + SA + DSPE-mPEG 2000	5.0	98 ± 11	15.1 ± 0.66	0.268 ± 0.013

[a] Dynamic light scattering (DLS) was used to measure the size and zeta potential of monensin (MON) intercalated in various liposomal formulations. The determined values are represented as the means ± standard deviations ($n = 3$).
[b] PDI, polydispersity index.

evaluate size distribution in two dimensions. The liposomal formulations predominantly consist of unilamellar vesicles in the size range of 90 to 120 nm, as observed in the TEM images. The two techniques (TEM analysis and DLS measurement) showed a similar pattern of particle size and spherical morphology, as shown in Fig. 1.

Effect of monensin in various conventional and sterically stabilized liposomal formulations on the growth of *P. falciparum* 3D7 *in vitro*. The effect of monensin in various liposomal formulations on the growth inhibition of asynchronous *P. falciparum* 3D7 in culture was evaluated by the inhibition of the incorporation of [^{3}H]hypoxanthine in parasites. It was observed that the efficacy of monensin significantly depended on the composition of lipids and different densities of DSPE-mPEG 2000 on the liposomal surface. The IC_{50}s for the growth of the parasites for liposomes with stearylamine, SPC:Chol, phosphatidic acid, and free monensin were found to be 0.74, 1.11, 2.98, and 3.17 nM, respectively (Fig. 2A). There was a significant reduction in parasite growth when monensin was delivered through stearylamine (SA) liposome, with 4.2-fold enhancement in antimalarial activity compared with that with free drug. However, placebo formulations without monensin/stearylamine had no antiplasmodial effects, whereas drug-free SA liposome exhibited an IC_{50} of 5.56 μM (data not shown). The developed formulations with monensin were superior to standard antimalarials, like chloroquine and artemisinin, displaying enhanced antimalarial activity (Fig. 2B). The incorporation of different densities (0.5, 2.5, and 5 mol%) of DSPE-mPEG 2000 on the surface of SPC:Chol and PA liposomes significantly enhanced the antimalarial activity of monensin compared to that in conventional forms. The IC_{50} for monensin in liposome containing SPC:Chol with 5 mol% PEG 2000 was 0.39 nM, showing a 2.8-fold reduction in antimalarial activity com-

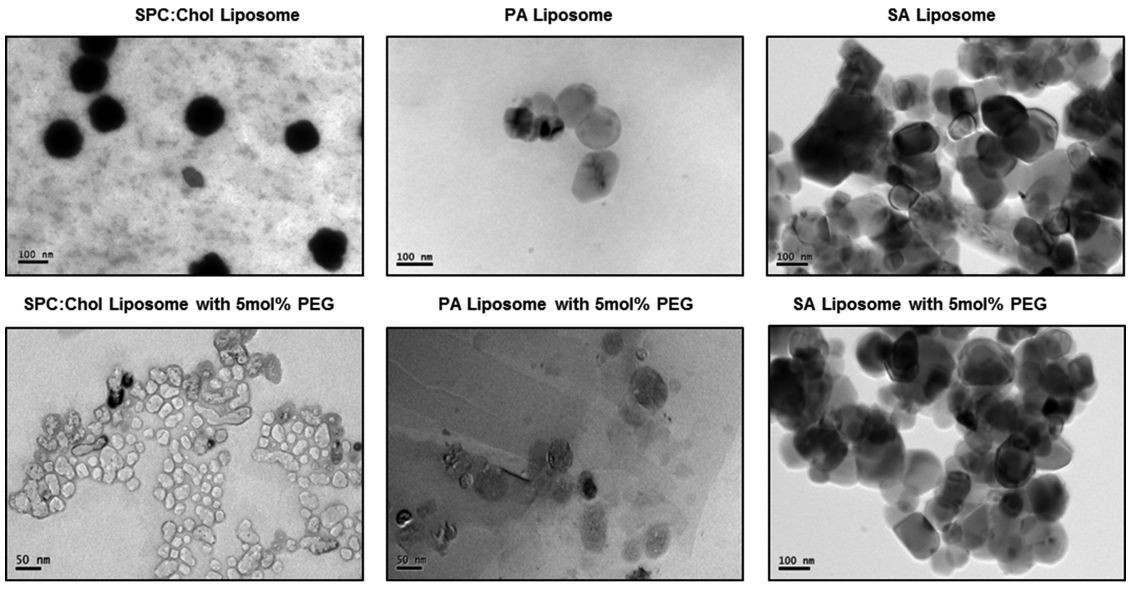

FIG 1 Characterization of various formulations of liposomes using high-resolution transmission electron microscopy (HRTEM). Representative images of various formulations of liposomes loaded with monensin are shown. The liposomes showed spherical morphology and size distribution, with a mean diameter of 90 to 120 nm.

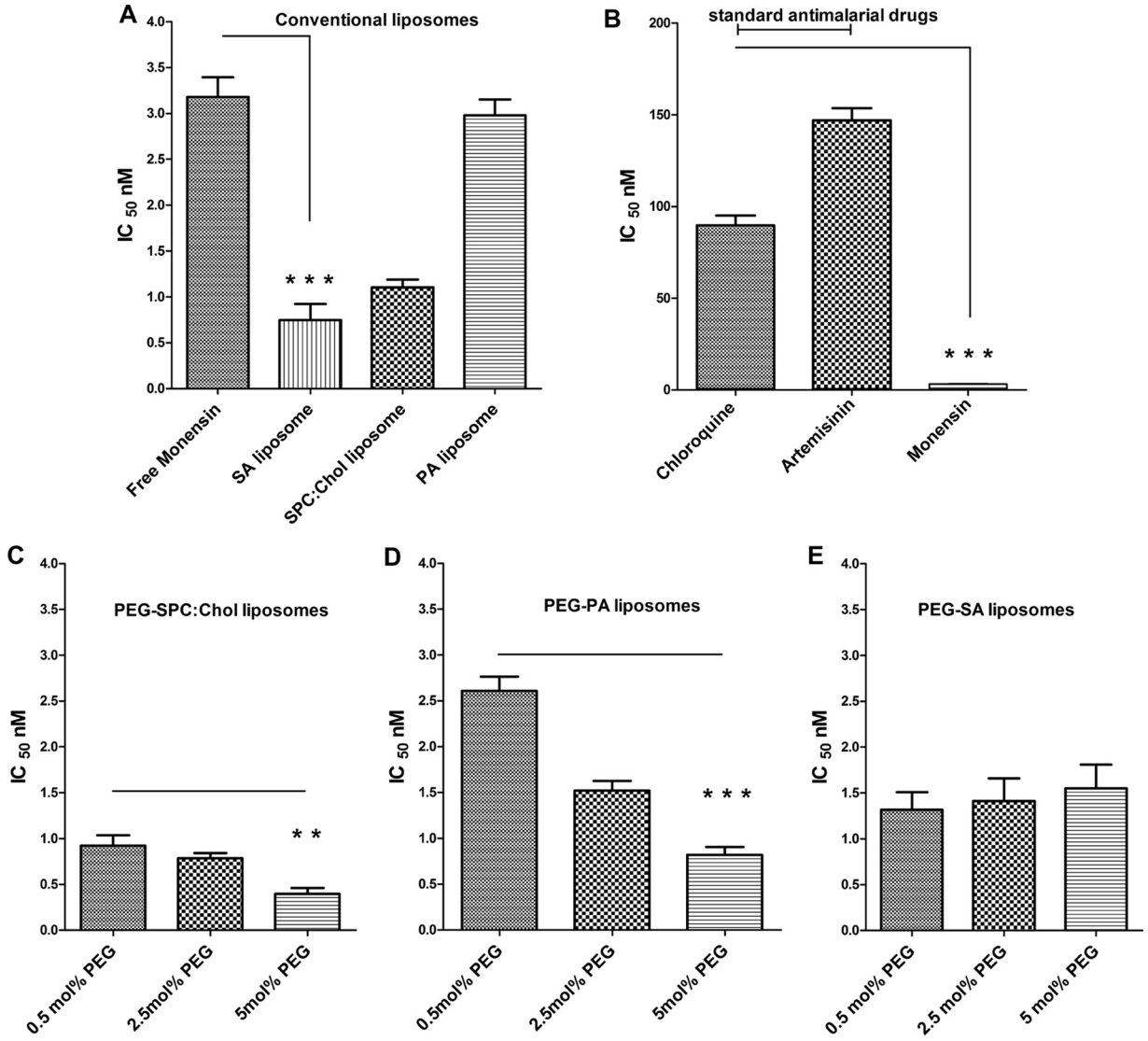

FIG 2 Effect of monensin in various conventional and sterically stabilized liposomal formulations on the growth inhibition of *P. falciparum* (3D7) in culture. (A) Formulations with SPC:Chol, PA, and SA (4% final hematocrit and 2% parasitemia) were incubated for 42 h at 37°C. ***, $P < 0.001$, Student's *t* test. (B) Effect of standard antimalarial drugs (CQ and ART). (C to E) Liposomal formulations with different densities of DSPE-mPEG 2000 (0.5, 2.5, and 5 mol%). The IC_{50}s were assessed by measuring the incorporation of [^{3}H]hypoxanthine in parasites, as described in the Materials and Methods. The data are represented as the means ± standard deviation (SD) from the results from three independent experiments. ***, $P < 0.0001$, ANOVA. **, $P < 0.001$.

pared with that with the SPC:Chol liposome (IC_{50}, 1.1 nM) formulation. Monensin in PA liposome with 5 mol% PEG 2000 (IC_{50}, 0.81 nM) showed a 2.7-fold reduction in antimalarial activity compared with PA liposome (IC_{50}, 2.98 nM) (Fig. 2C and D). On the other hand, monensin in positively charged SA liposome had no observable effect on the growth of parasites with an increase in PEG density, as shown in Fig. 2E. The maximum inhibition of growth of *P. falciparum* was observed when monensin was delivered through a PEGylated liposomal formulation (SPC:Chol) with 5 mol% DSPE-mPEG 2000 (Fig. 2C). There was no observable hemolysis in both normal and infected RBCs at effective concentrations of monensin in liposomes (data not shown). These results clearly indicate that the inhibition of growth of *P. falciparum* is dependent on different lipid compositions and densities of DSPE-mPEG 2000 on the liposomal surface.

Effect of liposomal monensin with or without SA with 5 mol% DSPE-mPEG 2000 in combination with free artemisinin on growth of different stages of *P. falciparum* 3D7 in culture. The antimalarial activity of monensin (MON) loaded in liposomes with or without SA with 5 mol% DSPE-mPEG 2000 in combination with free artemisinin (ART) was assessed in different developmental stages of parasites. As shown in Table 2, the combination of free MON plus ART at different ratios showed an additive interaction against 3D7, while monensin in SPC:Chol with 5 mol% PEG plus ART showed a reduction in IC_{50} with an increase in ART dose. We previously reported that stearylamine (SA) has antimalarial properties (36). Therefore, SA-bearing liposomal MON plus ART showed a more pronounced effect on parasiticidal activity compared with that in formulations without SA. ART alone at concentrations of 11, 22, 44.2, and 88.5 nM had a minimal killing effect.

TABLE 2 Effect of liposomal monensin with or without SA having 5 mol% PEG 2000 in combination with free artemisinin on growth of *P. falciparum* 3D7 in culture[a]

Drug combination	IC_{50}s (mean ± SD) after 42 h incubation (nM)		
	Asynchronized stage	Ring stage	Trophozoite and schizont stages
Free MON	3.27 ± 1.1	2.68 ± 0.34	1.86 ± 0.73
MON + ART 11 nM	2.45 ± 0.6	1.63 ± 0.42	0.74 ± 0.32
MON + ART 22 nM	1.78 ± 0.42	1.11 ± 0.21	0.44 ± 0.11
MON + ART 44.2 nM	1.4 ± 0.8	0.89 ± 0.39	0.29 ± 0.30
MON + ART 88.5 nM	1.25 ± 1.1	0.37 ± 0.76	<0.14
SPC:Chol liposome + 5 mol% PEG 2000	0.86 ± 1.3	1.04 ± 0.47	0.89 ± 0.13
SPC:Chol + PEG + MON + ART 11 nM	0.67 ± 0.9	0.95 ± 0.52	0.41 ± 0.19
SPC:Chol + PEG + MON + ART 22 nM	0.52 ± 0.8	0.77 ± 0.66	0.22 ± 0.23
SPC:Chol + PEG + MON + ART 44.2 nM	0.38 ± 1.3	0.56 ± 0.45	<0.14
SPC:Chol + PEG + MON + ART 88.5 nM	0.22 ± 0.75	0.268 ± 0.34	<0.14
SA liposome + MON + 5 mol% PEG 2000	1.63 ± 0.85	1.26 ± 0.20	0.76 ± 0.49
SA liposome + MON + ART 11 nM	0.89 ± 0.54	1.10 ± 0.18	0.31 ± 0.10
SA liposome + MON + ART 22 nM	0.31 ± 0.72	0.77 ± 0.4	0.17 ± 0.09
SA liposome + MON + ART 44.2 nM	<0.14	0.56 ± 0.11	<0.14
SA liposome + MON + ART 88.5 nM	<0.14	<0.14	<0.14

[a] Effect of liposomal monensin with or without SA having 5 mol% PEG 2000 in combination with free ART against asynchronous and synchronous culture (ring, trophozoite, and schizont stages) of *P. falciparum* (3D7) *in vitro*. A series of concentrations of monensin (4.65, 2.32, 1.16, 0.58, 0.29, and 0.14 nM) with ART were used. The IC_{50}s were assessed by measuring the incorporation of [^{3}H]hypoxanthine into nucleic acids of the parasites, as described in the Materials and Methods. The data are the means ± SD of the results from three independent experiments.

However, the observable impact on parasite growth was more prominent at the trophozoite and schizont stages than that at the ring stage. Notably, the intracellular delivery of liposomal monensin at a higher concentration to parasitophorous vacuoles of infected erythrocytes was attributed to strong antimalarial action in combination with free ART. Altogether, the combined therapy of SA-liposomal MON plus ART was found to be more effective on the developmental asexual life cycle of human malarial parasite.

Effect of different doses of monensin in various conventional liposomal formulations on *P. berghei* NK65 infection in Swiss albino mice. We assessed the antimalarial efficacy of monensin in free and liposomal forms using a modified version of Peter's 4-day suppressive test (37). A murine model of malaria was developed by intraperitoneal injection of 1×10^7 *P. berghei* NK65-infected erythrocytes. Monensin in various liposomal formulations was administered 48 h postinfection in mice. There was progressive decrease in parasitemia with increasing dose of monensin in different liposomal formulations (Fig. 3A). On day 15, in the untreated group, the parasitemia level was found to be 40 to 45%. Parasitemia in mice treated with 8 mg/kg free monensin was 30%, whereas it was 10% for SA liposome, 12.8% for SPC:Chol liposome, and 14.5% for PA liposome; representative blood smears are shown in Fig. 3C. However, the placebo formulations without monensin/stearylamine had no observable effect on the killing of parasites, whereas drug-free SA liposome at a dose of 5 mg/kg had marginal effect on the reduction of parasitemia to 37%. Therefore, the antimalarial properties of stearylamine in liposome in combination with monensin provokes enhanced killing of parasites. The median survival time of the treated group with SA liposome was 22.5 days, exhibiting a marked delay in death and survival, while that of the free-monensin-treated group was 16.5 days, and that of the untreated group was 15.5 days, as shown in Fig. 3B ($P < 0.0001$).

Effect of incorporation of different chain lengths of DSPE-mPEG in monensin-loaded liposomes on *P. berghei* NK65 infection in Swiss albino mice. It is well established that PEG can prolong the circulatory life of liposomes and that it depends on the surface density of the polymer and molecular weight (MW) of different PEG chain length on the surface of liposomes (38). The surface charge of PEGylated liposomes can be changed by varying the surface density and chain length of PEG. We have evaluated the effect of variations in PEG chain length (750, 1000, 2000, 3000, and 5000) with 2.5 mol% MW on the SPC:Chol liposomal monensin (8 mg/kg) of four doses against infected mice. On day 15 postinfection, there was progressive suppression at parasitemia levels of 16%, 13%, and 6% with increase in PEG chain length (750, 1000, and 2000, respectively). In contrast, high-MW chain length (PEG 3000 and PEG 5000) had parasitemia levels of 14% and 22%, respectively, compared with the untreated group (40 to 45%) (Fig. 4A). The maximum reduction in parasitemia and clearance of parasite from the blood was found with the DSPE-mPEG 2000 chain length. The median survival times of animals treated with different chain lengths of DSPE-mPEG, 750, 1000, 2000, 3000, and 5000, were 21, 22, 24.5, 22, and 20.5 days, respectively. The chain length of DSPE-mPEG 2000 extended the survival compared with other chain lengths, as shown in Fig. 4B ($P < 0.05$).

Effect of monensin in various liposomal formulations with or without SA with different densities of DSPE-mPEG 2000 on *P. berghei* NK65 infection in Swiss albino mice. Based on the above-mentioned results, the PEG 2000 chain length was found to be optimum, with maximum efficacy in delivering monensin intracellularly, where the parasite resides in the RBCs. Therefore, the antimalarial efficacy of monensin intercalated in various liposomal formulations with different densities of PEG 2000 was studied in *P. berghei*-infected mice, as shown in Fig. 5A. The infected mice were treated with four doses of 8 mg/kg in various liposomes loaded with monensin having different densities of PEG 2000. It was observed that the variation in PEG density significantly modulated the efficacy of monensin in liposomes in killing the parasites. Figure 5A shows the parasitemia on day 15 postinfection for

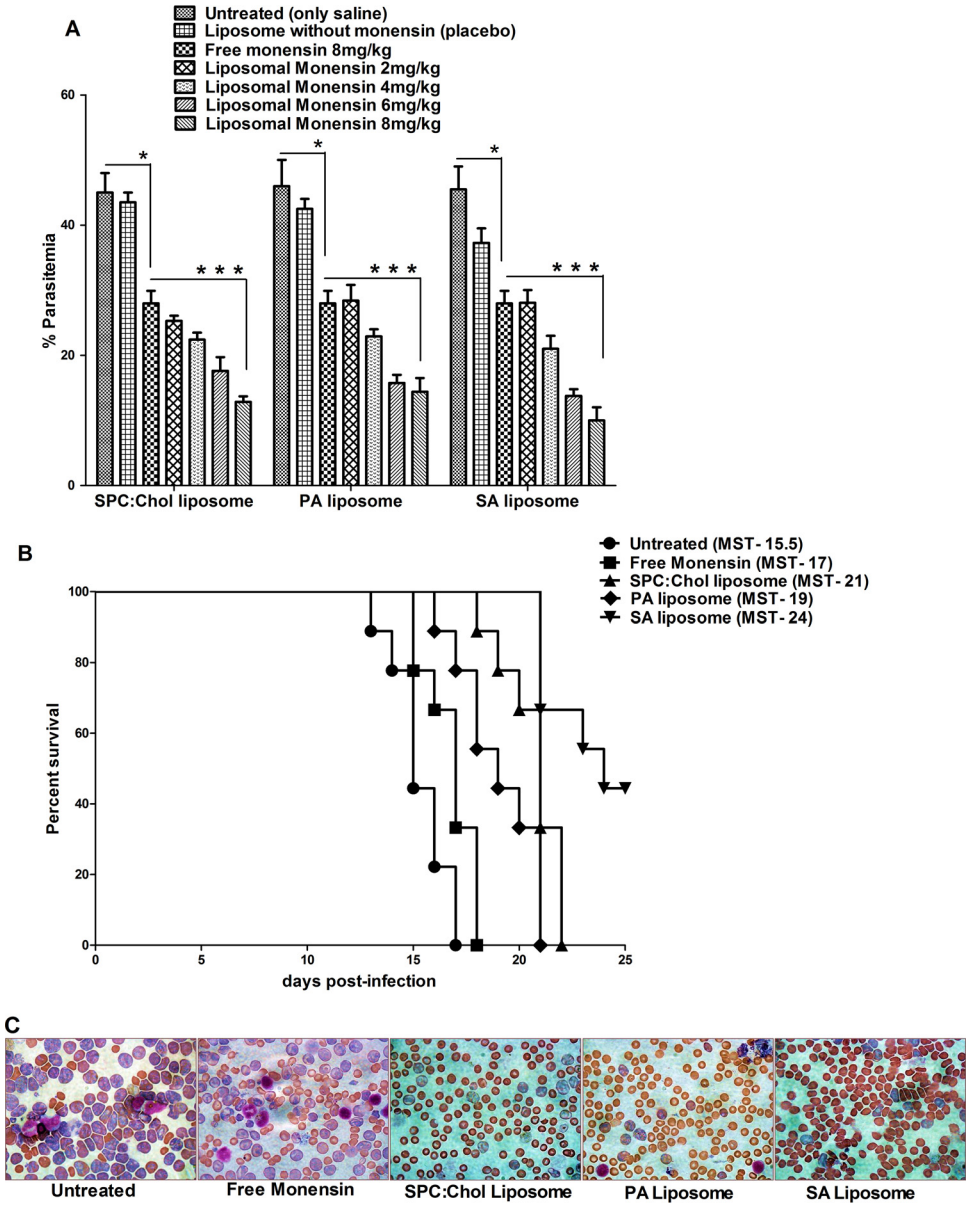

FIG 3 Effect of different doses of monensin in conventional liposomes on parasitemia and survival of *P. berghei* NK65-infected Swiss albino mice. (A) Free monensin and monensin-containing liposomal formulations (SPC:Chol, PA, and SA) were administered subcutaneously. The untreated group was administered saline. The data represent the means ± SD, with 9 animals in each group. (B) Survival of various liposomal formulations of monensin in treatment groups compared to that with free monensin. The median survival time (MST) (in days) of the animals in each group is shown in parentheses. (C) Photomicrograph of blood smears of untreated versus treatment groups at day 15 postinfection, shown at 100× magnification. For the determination of parasitemia in blood smears, 10 different random optical fields were counted and parasitemia calculated using the Cell Counting Aid software. ***, $P < 0.0001$, ANOVA; ***, $P < 0.001$, Student's *t* test. *, $P < 0.01$.

the untreated group and liposomal formulations with different densities of PEG (0.5, 2.5, and 5 mol%) in SA liposome, SPC:Chol liposome, and PA liposome. All formulations exhibited a progressive decrease in parasite load with an increase in PEG density; representative blood smears are shown in Fig. 5C. However, monensin-loaded SA liposome with maximum PEG density (5 mol%) was the most effective, followed by SPC:Chol liposome with 5 mol% PEG. These results clearly underscore the role of lipid composition and optimal PEG density in improving the delivery of monensin in stearylamine liposome and consequent enhancement of efficacy against *P. berghei* infection. The median survival time of animals treated with PEGylated formulations (at 5 mol%) for SA liposome was 27.5 days, whereas that with SPC:Chol liposome was 23.5 days, and that with PA liposome was 22 days (Fig. 5B) ($P < 0.01$).

Histopathological analysis. The *P. berghei* NK65 infection in mice reached parasitemia levels ranging from 40 to 45% on day 15 postinfection. The histopathological analysis of liver sections of the untreated group showed a heavy deposit of hemozoin pigment in Kupffer cells and periportal inflammatory cell infiltration. All

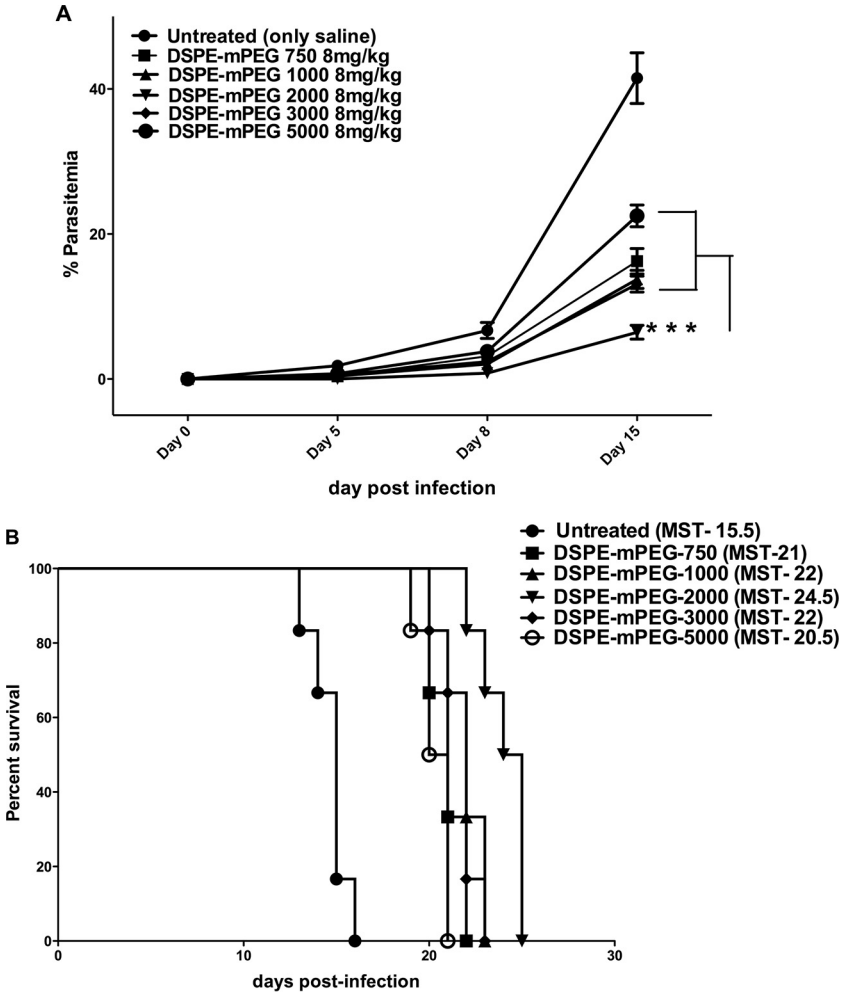

FIG 4 (A) Effect of monensin in SPC:Chol liposome with 2.5 mol% of different chain lengths of DSPE-mPEG on parasitemia and survival of *P. berghei* NK65-infected Swiss albino mice. Each group was injected with 8 mg/kg of body weight of monensin in liposomal formulations with various chain lengths of PEG MW (750, 1000, 2000, 3000, and 5000). The untreated group was given saline. The data represent the means ± SD, with 9 animals in each group. (B) Survival of mice treated with various liposomal formulations of monensin having different chain lengths of DSPE-mPEG. Analysis was done as described in the Fig. 3 legend. ***, $P < 0.0001$.

treatment groups were given four doses of 8 mg/kg monensin in various formulations of liposomes. The free-monensin-treated group exhibited patterns of hemozoin deposit and inflammation similar to those of the untreated group. In contrast, liver samples from treatment groups with various conventional liposomal formulations exhibited a decrease in hemozoin pigment with reduced liver damage. Noticeably, the treatment group administered with liposomes with 5 mol% PEG 2000 displayed a marked reduction in hemozoin pigment with well-preserved liver morphology in comparison to the uninfected group, as shown in Fig. 6. There was no observable pathological damage in liver (hepatomegaly), and there was a reduced parasite burden in all PEGylated liposomal formulation treatment groups. Therefore, our results show that PEGylated liposomes are highly effective in reducing the liver damage caused by *P. berghei* infection.

Effect of liposomal monensin with or without SA with 5 mol% DSPE-mPEG 2000 in combination with free artemisinin on *P. berghei*-infected mice. Stearylamine-bearing cationic liposomal monensin and SPC:Chol liposomal monensin at different doses (4 mg/kg and 6 mg/kg of body weight) with 5 mol% PEG 2000 was shown to have better efficacy in clearing the parasite burden in than other formulations. This led us to evaluate its efficacy in combination with free artemisinin (ART) at different doses (10, 20, or 40 mg/kg of body weight) in both strains of rodent malaria *P. berghei* ANKA and NK65 (Fig. 7A and B). Different doses of each formulation of liposomal monensin were coadministered with different doses of free ART to infected mice. On day 15, there was a significant reduction in parasitic burden at a higher dose of free ART (40 mg/kg) coadministered with PEGylated SA liposome or PEGylated SPC:Chol liposome containing monensin (at 4 mg/kg or 6 mg/kg) compared to that with the untreated group (Fig. 7A). All animals exhibited severe neurological symptoms and succumbed to death on days 8 to 10 (Fig. 7A). Interestingly, a similar pattern was observed with *P. berghei* NK65 infection, which triggers a high level of blood-stage parasitemia in mice (Fig. 7B). None of the drugs alone at the indicated doses completely cleared parasitemia. In contrast, PEGylated SA liposomal monensin in combination with ART (5 mg/kg SA + 6 mg/kg MON + 40 mg/kg

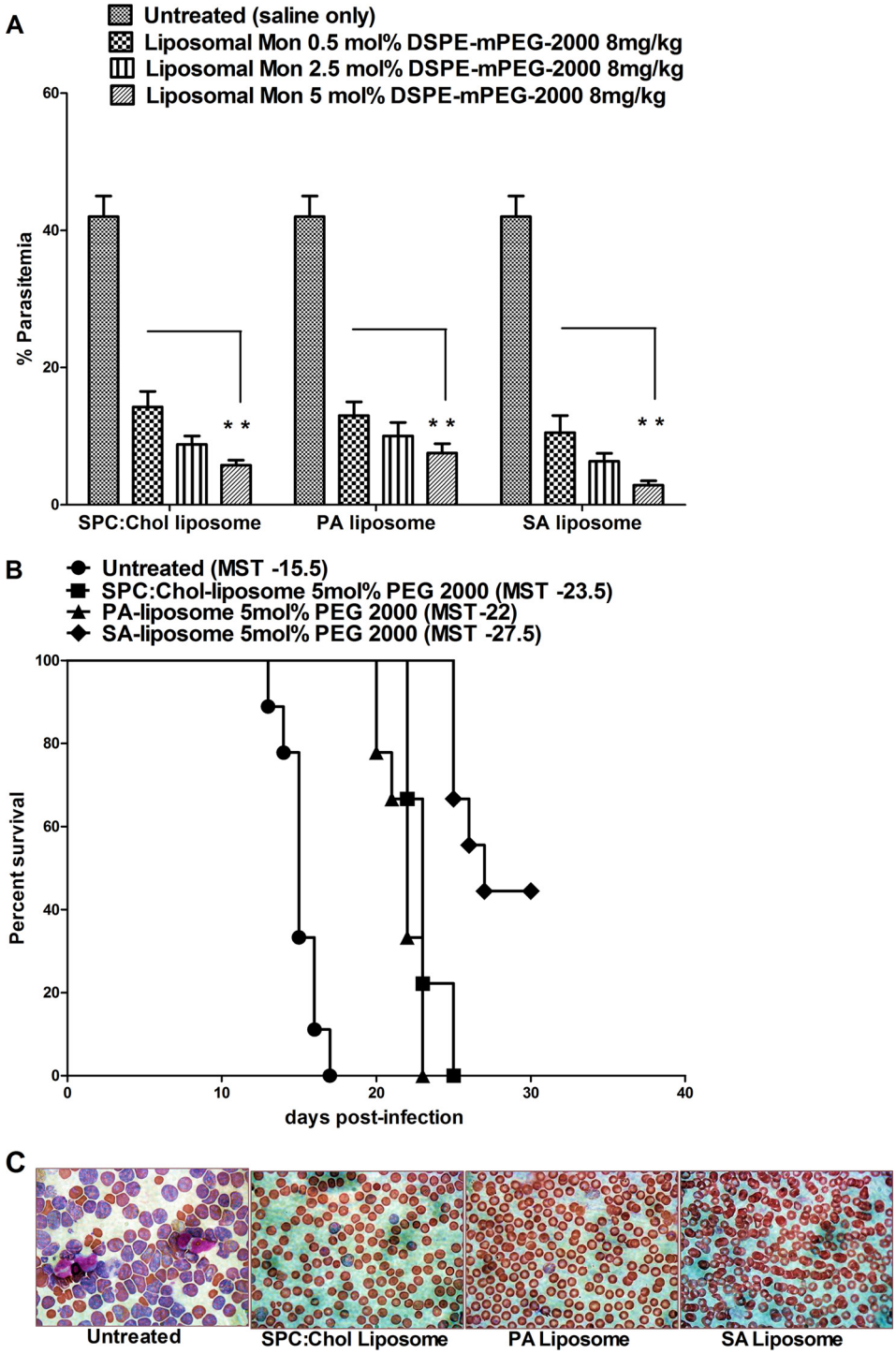

FIG 5 Effect of monensin in various liposomal formulations with different densities of DSPE-mPEG 2000 on parasitemia and survival of *P. berghei* NK65-infected Swiss albino mice. (A) Mice in each group were injected subcutaneously with 8 mg/kg of various formulations having different lipid compositions and PEG 2000 densities (0.5, 2.5, and 5 mol%). The data represent the means ± SD of 9 animals in each group. (B) Survival of mice treated with various liposomal formulations of monensin. The analysis was done as described in the Fig. 3 legend. (C). Photomicrograph of blood smears of untreated versus treatment groups at day 15 postinfection shown at 100× magnification. Parasitemia was determined as described in the Fig. 3 legend. **, $P < 0.001$.

ART) significantly enhanced the efficacy by reducing the parasite load in both strains of *P. berghei* with 100% survival (Fig. 7C) ($P < 0.0001$). In addition, a significant reduction in parasitemia levels was observed at lower doses of ART (10 mg/kg and 20 mg/kg) in combination with monensin in liposomal formulations in both strains ($P < 0.0001$). Therefore, these results suggest that liposomal monensin in combination with artemisinin enhances therapeutic efficacy in both *Plasmodium* strains.

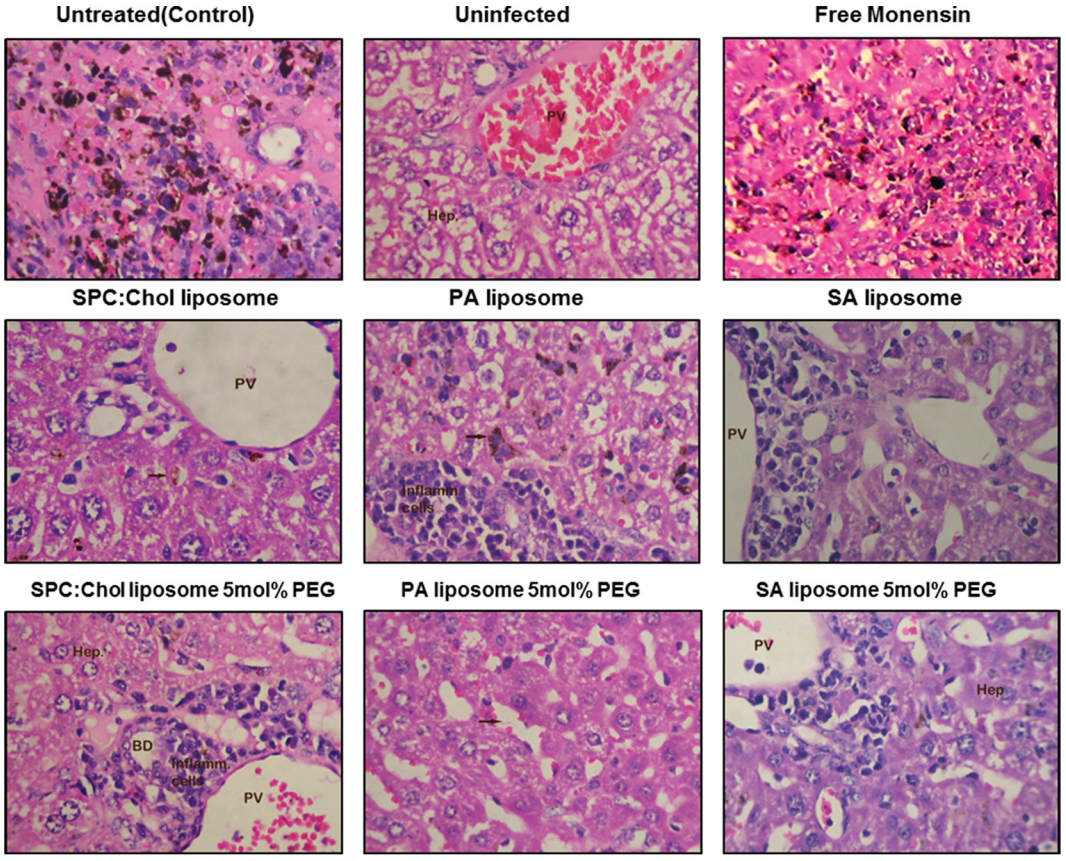

FIG 6 Histopathology of livers of mice infected with *P. berghei* NK65 at day 15 postinfection. Representative 400× photomicrographs of hematoxylin and eosin (H&E)-stained 5-mm sections of liver are shown. All treatment groups were administered four doses at 8 mg/kg, as described in the Materials and Methods. In the untreated group, mice infected with *P. berghei* displayed similar tissue damages as free monensin treated group with heavy deposition of hemozoin pigment and inflammation. The group treated with conventional liposomes demonstrates reduction in pigment. The group treated with 5 mol% PEG 2000 of all formulations exhibited significant reduction in malarial pigment and retained normal morphology compared with uninfected mice. PV, portal vein; Hep, hepatocyte; PT, portal triad; CV, central vein; BD, bile duct.

Assessment of plasma clearance and biodistribution of monensin in conventional and sterically stabilized liposomal formulations using fluorescent surface marker NBD-PC. It is evident from the above-mentioned results that the clearance of parasitemia by various formulations of liposomal monensin depends on the lipid dose, lipid composition, and density of PEG layer on the surface. The differential action of monensin (in various liposomal formulations) might be due to the variation in the extent of the release of liposomes from the site of injection to the blood and distribution to various organs (liver, spleen, lung, kidneys, and brain). Therefore, we investigated the retention of liposomes in plasma and different tissues at different time intervals after subcutaneous administration in uninfected and infected mice (30 to 35% parasitemia) of *P. berghei* NK65. In this study, conventional liposomes and sterically stabilized liposomes with 5 mol% PEG 2000 were labeled with fluorescent lipid NBD-PC (1 mol%) as a marker for detection, as shown in Fig. 8A. In normal mice, the formulation of SPC:Chol liposome in plasma reached a peak level after 4 h of injection and declined rapidly thereafter. In contrast, SPC:Chol liposome with 5 mol% PEG 2000 showed a peak between 4 and 12 h with a progressive decrease in fluorescence intensity and remained in the blood for up to 24 h. However, PA liposome and SA liposome attained a peak at 1 to 2 h and remained in the blood until 12 h with a reduced fluorescence signal. A similar pattern was observed in *P. berghei*-infected mice. Notably, higher fluorescence intensity was observed in the whole-blood pellets of infected mice than that in normal mice (data not shown). However, PEG liposomes showed 2-fold enhanced retention in the liver at 4 h compared with conventional formulations in infected mice (Fig. 8B). Overall, the longevity of PEGylated formulations with a maximum density of PEG (5 mol%) was retained in blood circulation, which strongly correlates with a pharmacological effect in clearing parasitemia compared with conventional formulations.

***In vitro* and *ex vivo* uptake of fluorescently tagged liposomal formulations by different stages of *P. falciparum* in culture and *P. berghei*-infected erythrocytes.** To determine the uptake of SA liposome and PEGylated liposome in infected erythrocytes and uninfected erythrocytes, the intracellular concentrations of coumarin-6 (C-6)-labeled liposomes were measured in asynchronized culture at different time intervals, as shown in Fig. 9A. Under *in vitro* conditions, fluorimetric analysis showed that the level of intracellular fluorescence increased with time, and maximum uptake was observed at 4 h. Fluorescence microscopy showed that nanosized C-6-labeled liposome alone (Fig. 9B) and dually labeled fluorescent liposome (R18 and calcein) (Fig. 9C) were preferentially colocalized inside infected erythrocytes compared with un-

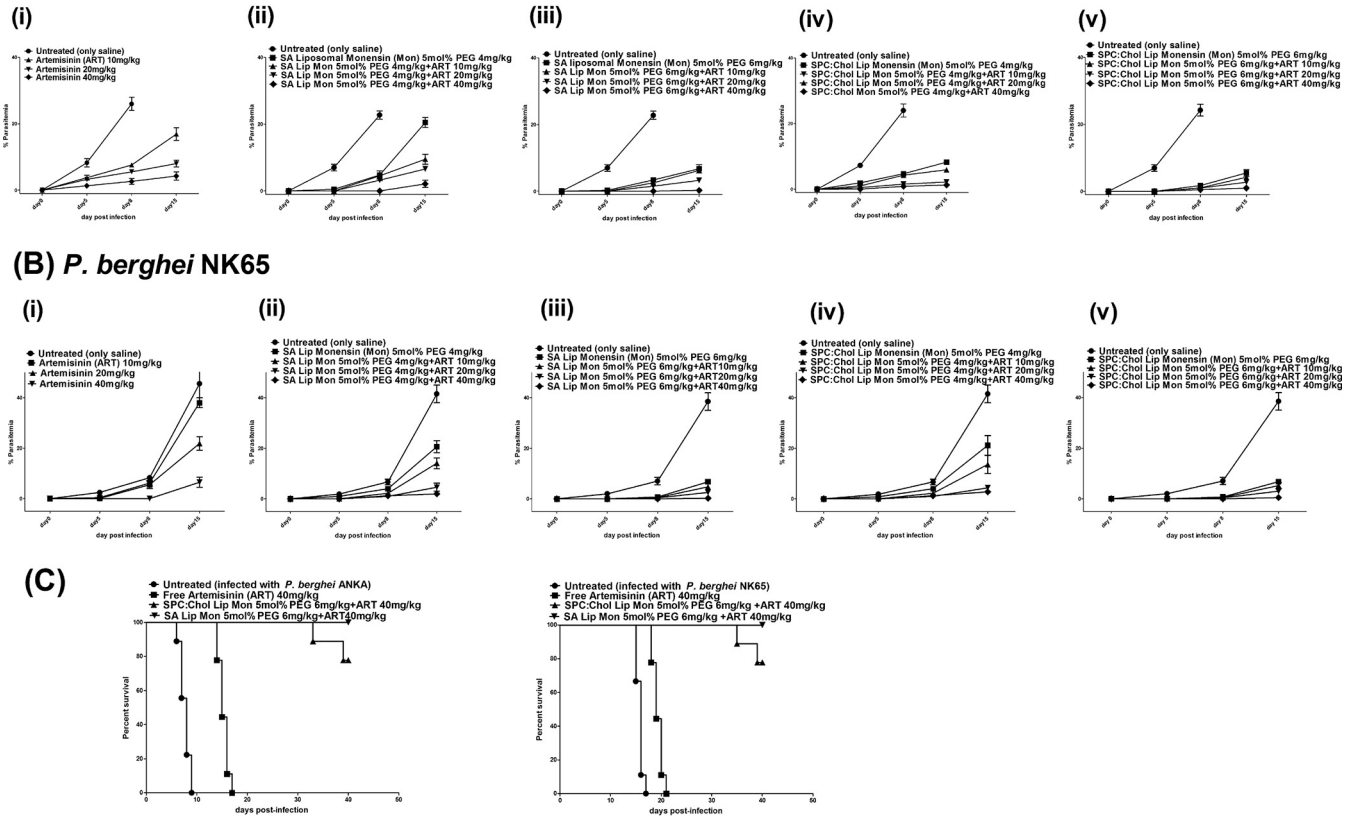

FIG 7 Effect of combined treatment of monensin (4 mg/kg or 6 mg/kg) in SA liposome-PEG 2000 (5 mol%) or SPC:Chol-PEG 2000 (5 mol%) alone or in combination with free artemisinin (10, 20, or 40 mg/kg) on parasitemia and survival of *P. berghei* ANKA and *P. berghei* NK65 in mice models. Mice infected with 1×10^7 *P. berghei*-infected RBCs after 48 h postinfection were treated subcutaneously with four consecutive days of liposomal formulations. The untreated group was injected with PBS, and the % parasitemia was determined by blood smear on days 5, 8, and 15 postinfection. (A and B) Artemisinin (ART) alone (i), coadministration of SA liposomal monensin with DSPE-mPEG 2000 with free ART (ii and iii), coadministration of SPC:Chol liposomal monensin with DSPE-mPEG 2000 with free ART (iv and v). The data are the means ± SEM from nine animals per treatment group. (C) Survival of mice in treatment groups ($n = 9$) with ART alone and in combination with monensin in different formulations. Lip, liposome.

infected ones. Under *ex vivo* conditions, a similar pattern was observed with preferable localization in *P. berghei*-infected mouse erythrocytes compared with uninfected RBCs (Fig. 9B and C).

DISCUSSION

Our results clearly demonstrate the antimalarial activities of various liposomal formulations composed of natural lipids, making them a suitable delivery vehicle for monensin under *in vitro* and *in vivo* conditions. The liposomal formulations of monensin developed in this study have efficacy superior to that of free monensin. We observed that free monensin and various formulations of liposomal monensin are highly potent compared with standard antimalarials (artemisinin and chloroquine) (Fig. 2). The antimalarial activity of monensin may be due to the alkalinization of parasite food vacuoles (12–14) and the induction of eryptosis, which leads to cell membrane scrambling and cell shrinkage in infected erythrocytes (39). As reported earlier, free monensin does not cause any hemolytic activity up to a concentration of 10 μM in uninfected RBCs (39). This suggests that the inhibitory effect of various formulations of monensin toward infected RBCs is independent of hemolysis. The degree of specificity of monensin toward the antimalarial activity of infected erythrocytes has been studied using lipid membrane models (40). Our results indicate that the enhanced antimalarial efficacy of monensin in liposomal formulations is due to preferential internalization of liposomes by parasitized RBCs (Fig. 9). The preferential interaction of liposome with infected erythrocytes might be due to a decrease in surface pressure that promotes its cellular uptake.

There was considerable suppression of parasitemia when monensin was administered in stearylamine liposomes (Fig. 3). Positively charged stearylamine has been shown to induce the release of intravesicular contents when fused with the erythrocyte membrane (41). Nonselective binding of SA liposome toward normal erythrocytes is due to a negatively charged RBC surface membrane composed of sialylated glycoproteins (42). The enhancement in adsorption or binding of liposomes to infected erythrocytes may be facilitated by the electrostatic interaction of positively charged SA liposomes with the negatively charged surface of infected RBCs that have elevated levels of phosphatidylserine (PS) on the outer membrane (43). This interaction may lead to membrane disruption and cell death. This is in agreement with our previous report that showed that SPC-stearylamine liposomes alone without monensin inhibited the growth of *P. falciparum* in culture (36).

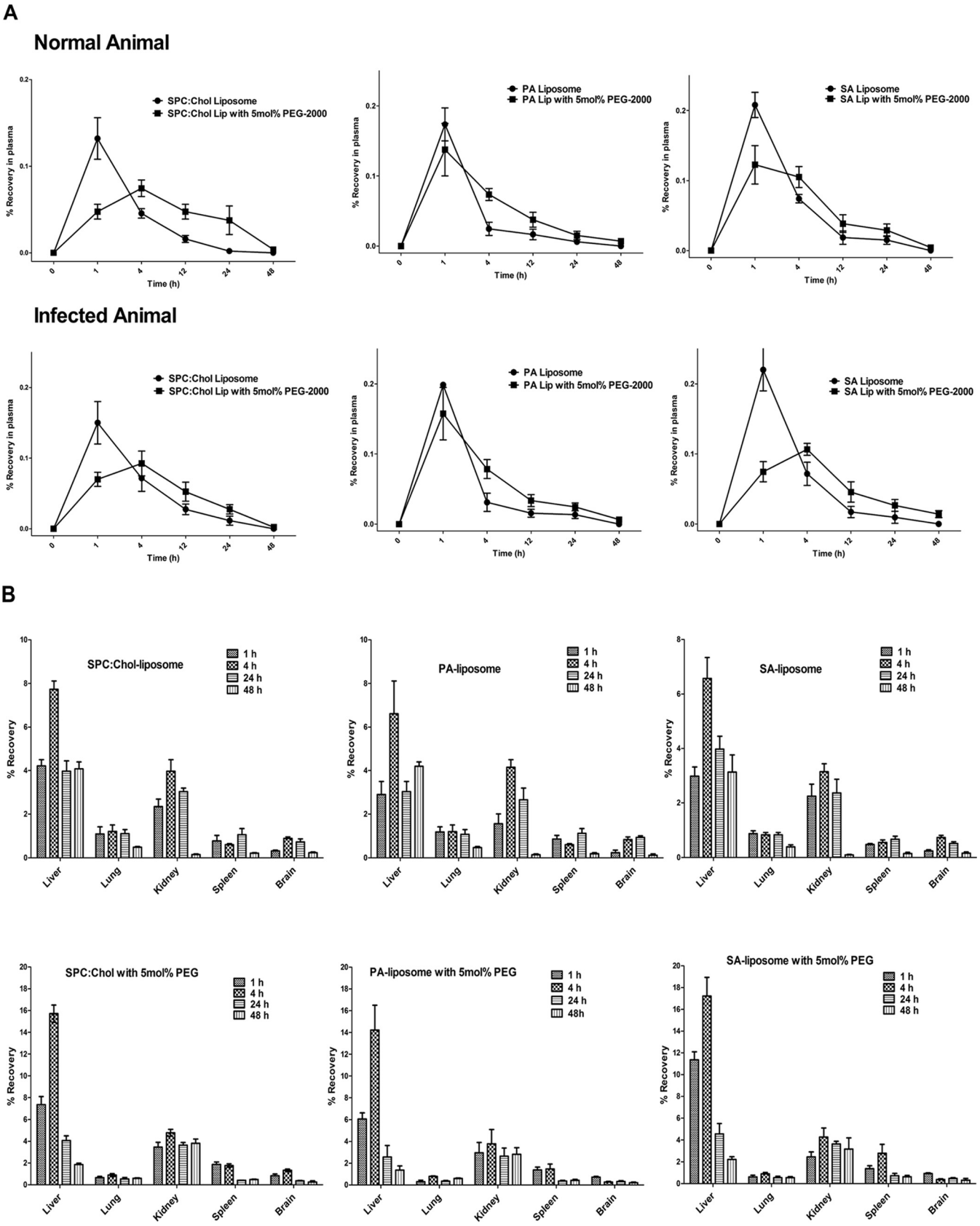

FIG 8 Plasma clearance and biodistribution of fluorescently labeled NBD-PC in various formulations of monensin. (A) Liposomal formulations were administered subcutaneously in normal and infected mice (30 to 35% parasitemia). Mice were sacrificed, blood was drawn through cardiac puncture at various time intervals (1, 4, 12, 24, and 48 h) after the administration, and fluorescence intensity was measured as described in the Materials and Methods. (B) Biodistribution of NBD-PC-labeled liposomes in *P. berghei* NK65-infected mice. Each point represents the mean ± SD from the results with three mice.

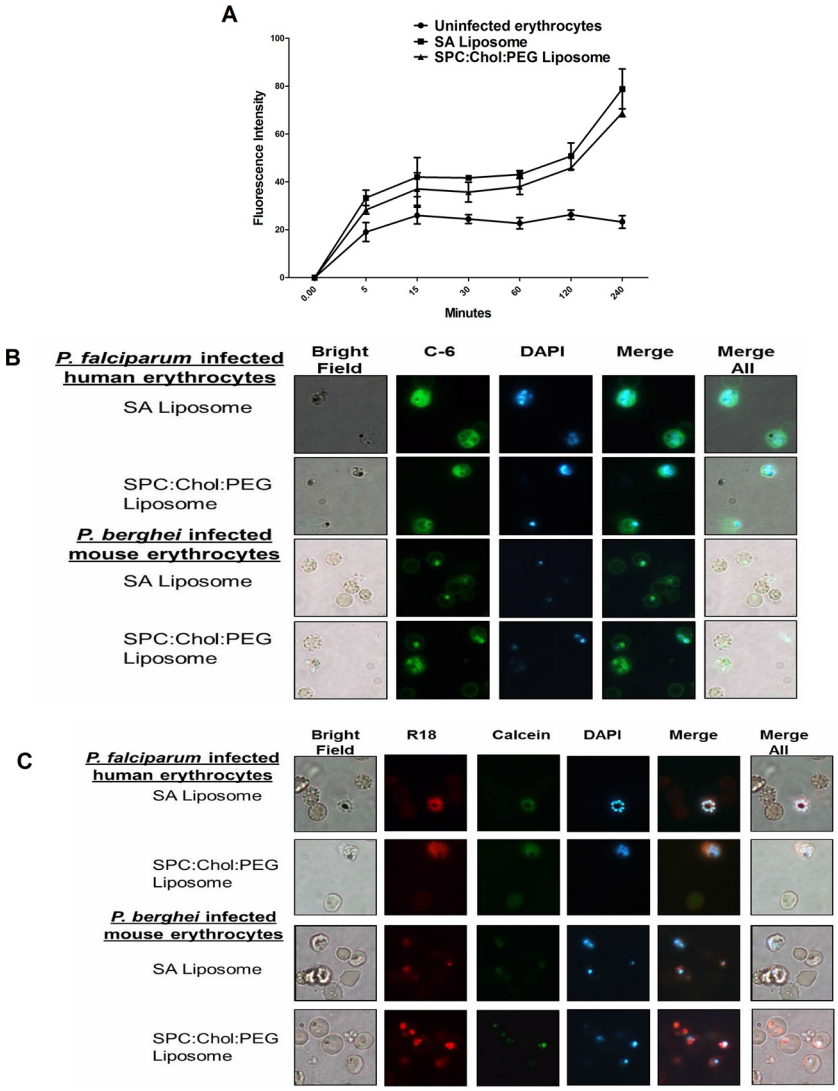

FIG 9 Uptake of fluorescently labeled liposomal formulations by *P. falciparum*- and *P. berghei*-infected erythrocytes. (A) Coumarin-6 (C-6)-labeled liposomes were added to a culture of *P. falciparum*. The internalization of liposomes was measured quantitatively at different time intervals using fluorescence spectrometry. (B) Localization of fluorescently labeled C-6 liposome in the parasites. (C) Accumulation of dually labeled fluorescent liposomes (octadecylrhodamine [R18] and calcein) in infected RBC nuclei was detected by fluorescence microscopy at 100× magnification. DAPI stains the *Plasmodium* nuclei (blue), coumarin-6 (green), R18 (red), and calcein (green).

We have shown that the circulatory life of monensin can be substantially modulated using polyethylene glycol-modified lipids without causing toxicity (Fig. 4 and 5). It has been reported that the interaction of liposomes with mammalian cells is highly dependent on the surface charge, PEG density, and chain length (44). An increase in PEG density from 0.5 to 5 mol% plays a significant role by hindering the attraction of serum proteins (opsonins), and the thickness of the polymer layer further decreases the uptake by macrophages, thereby enhancing circulation time (45). Surface modification of liposomes with PEG lipids of different molecular weights (i.e., chain length) has been shown to prolong circulation time in the blood and prevent their uptake by the liver and spleen (46, 47). Our results showed that modifying the liposomal surface structure with different densities of DSPE-mPEG 2000 enhanced the antimalarial efficacy of liposomal formulations compared with that of free monensin. Our biodistribution studies with fluorescently labeled liposomes demonstrate that an increase in PEG density from 0.5 to 5 mol% on the liposomal surface prolongs their circulatory life in the blood (Fig. 8A). Therefore, the incorporation of PEG by varying its density on the surface can significantly increase its circulation time, modulate the release profile of the drug at the site of infection, and facilitate greater interaction with infected RBCs, resulting in the suppression of parasitemia to a greater extent (48). These results are consistent with an earlier study that showed that the addition of PEG moiety facilitates an enhancement of fusion capacity to *P. berghei*-infected erythrocytes in the presence of Ca^{2+} with lesser interaction with normal RBCs (49). Our results indicate that interaction of PEG-grafted liposomes with infected RBCs depends on the density of polymer (mol%) and optimal chain length (Fig. 4). This is in agreement with a report that shows that the increase in PEG density disrupts the integrity and stability of the lipid membranes (48). Evidence suggests that excess PEGylation can inhibit cellular uptake, thereby reducing therapeutic potential (50).

It appears that liposomes with prolonged circulatory lives are efficient in delivering monensin to parasite-infected erythrocytes under *in vivo* conditions. These observations are also in agreement with a previous study in which recombinant human tumor necro-

sis factor alpha (rhTNF-α) in stealth liposomes has enhanced protective efficacy against *P. berghei* experimental cerebral malaria (51). We have demonstrated here that there is variation in the antimalarial activity of monensin in various liposomal formulations on *P. berghei* infection (Fig. 3). This may be due to variations in the drainage from the lymphatic system to the blood, clearance from plasma, and tissue distribution. In addition, there may be differences in the rate of uptake of liposomes in various tissues due to differences in blood flow in the liver and spleen and enhanced clearance of senescent and parasitized RBCs in heavily infected mice compared with healthy animals (Fig. 8B). Furthermore, there is enhanced uptake of liposomes in brain tissue under infected conditions (Fig. 8B), which might be effective in treating cerebral malaria during *P. falciparum* infection.

Our results demonstrate that there is a complete elimination of parasite burden by combination therapy of SA-bearing liposomal monensin with 5 mol% PEG with ART. To our knowledge, this is the first report that demonstrates that the coadministration of stearylamine, monensin, and artemisinin has enhanced antiplasmodial activity. In addition, artemisinin-based combination therapy (ACT) with PEGylated SA-bearing cationic liposomal monensin presents a profound additive interaction in killing *P. falciparum* in culture and is highly efficacious against *P. berghei* infection in a mouse model (Fig. 7). Therefore, we propose that our liposomal formulations containing stearylamine with DSPE-mPEG 2000 may provide a novel strategy to deliver potent hydrophobic antimalarials in combination with antimalarials, such as artemisinin, to overcome drug resistance in *P. falciparum* and prevent malaria relapse.

ACKNOWLEDGMENTS

This work was supported by a Delhi University Department of Science and Technology purse grant, an R&D grant from Delhi University, and ICMR project funding, Government of India, to P.C.G. V.R. was supported by the University Grant Commission and Council for Scientific and Industrial Research.

We thank C. R. Pillai (National Institute of Malaria Research, New Delhi, India) for providing rodent strains of *P. berghei* NK65 and ANKA and the Rotary Blood Bank, New Delhi, India, for a continuous supply of O+ blood. We thank Ashok Mukherjee for histopathological analysis of the samples. We also thank Manendra Pachuari, Richi V. Mahajan, and Lakshmi Narayana Kashyap for critical reading of the manuscript and for excellent technical help.

We declare no financial conflicts of interest.

REFERENCES

1. **Lim P, Wongsrichanalai C, Chim P, Khim N, Kim S, Chy S, Sem R, Nhem S, Yi P, Duong S, Bouth DM, Genton B, Beck HP, Gobert JG, Rogers WO, Coppee JY, Fandeur T, Mercereau-Puijalon O, Ringwald P, Le Bras J, Ariey F.** 2001. Decreased *in vitro* susceptibility of *Plasmodium falciparum* isolates to artesunate, mefloquine, chloroquine, and quinine in Cambodia from to 2007. Antimicrob Agents Chemother **54:**2135–2142.
2. **Wongsrichanalai C, Sibley CH.** 2013. Fighting drug-resistant *Plasmodium falciparum*: the challenge of artemisinin resistance. Clin Microbiol Infect **19:**908–916.
3. **Fairhurst RM, Nayyar GM, Breman JG, Hallett R, Vennerstrom JL, Duong S, Ringwald P, Wellems TE, Plowe CV, Dondorp AM.** 2012. Artemisinin-resistant malaria: research challenges, opportunities, and public health implications. Am J Trop Med Hyg **87:**231–241.
4. **Miotto O, Almagro-Garcia J, Manske M, Macinnis B, Campino S, Rockett KA, Amaratunga C, Lim P, Suon S, Sreng S, Anderson JM, Duong S, Nguon C, Chuor CM, Saunders D, Se Y, Lon C, Fukuda MM, Amenga-Etego L, Hodgson AV, Asoala V, Imwong M, Takala-Harrison S, Nosten F, Su XZ, Ringwald P, Ariey F, Dolecek C, Hien TT, Boni MF, Thai CQ, Amambua-Ngwa A, Conway DJ, Djimde AA, Doumbo OK, Zongo I, Ouedraogo JB, Alcock D, Drury E, Auburn S, Koch O, Sanders M, Hubbart C, Maslen G, Ruano-Rubio V, Jyothi D, Miles A, O'Brien J, Gamble C, Oyola SO, et al.** 2013. Multiple populations of artemisinin-resistant *Plasmodium falciparum* in Cambodia. Nat Genet **45:**648–655. http://dx.doi.org/10.1038/ng.2624.
5. **St. Laurent B, Miller B, Burton TA, Amaratunga C, Men S, Sovannaroth S, Fay MP, Miotto O, Gwadz RW, Anderson JM, Fairhurst RM.** 2015. Artemisinin-resistant *Plasmodium falciparum* clinical isolates can infect diverse mosquito vectors of Southeast Asia and Africa. Nat Commun **6:**8614. http://dx.doi.org/10.1038/ncomms9614.
6. **Mbengue A, Bhattacharjee S, Pandharkar T, Liu H, Estiu G, Stahelin RV, Rizk SS, Njimoh DL, Ryan Y, Chotivanich K, Nguon C, Ghorbal M, Lopez-Rubio JJ, Pfrender M, Emrich S, Mohandas N, Dondorp AM, Wiest O, Haldar K.** 2015. A molecular mechanism of artemisinin resistance in *Plasmodium falciparum* malaria. Nature **520:**683–687. http://dx.doi.org/10.1038/nature14412.
7. **Ashley EA, Dhorda M, Fairhurst RM, Amaratunga C, Lim P, Suon S, Sreng S, Anderson JM, Mao S, Sam B, Sopha C, Chuor CM, Nguon C, Sovannaroth S, Pukrittayakamee S, Jittamala P, Chotivanich K, Chutasmit K, Suchatsoonthorn C, Runcharoen R, Hien TT, Thuy-Nhien NT, Thanh NV, Phu NH, Htut Y, Han KT, Aye KH, Mokuolu OA, Olaosebikan RR, Folaranmi OO, Mayxay M, Khanthavong M, Hongvanthong B, Newton PN, Onyamboko MA, Fanello CI, Tshefu AK, Mishra N, Valecha N, Phyo AP, Nosten F, Yi P, Tripura R, Borrmann S, Bashraheil M, Peshu J, Faiz MA, Ghose A, Hossain MA, Samad R, et al.** 2014. Spread of artemisinin resistance in *Plasmodium falciparum* malaria. N Engl J Med **371:**411–423. http://dx.doi.org/10.1056/NEJMoa1314981.
8. **Bharti AR, Saravanan S, Madhavan V, Smith DM, Sharma J, Balakrishnan P, Letendre SL, Kumarasamy N.** 2012. Correlates of HIV and malaria co-infection in southern India. Malar J **11:**306. http://dx.doi.org/10.1186/1475-2875-11-306.
9. **Petersen I, Eastman R, Lanzer M.** 2011. Drug-resistant malaria: molecular mechanisms and implications for public health. FEBS Lett **585:**1551–1562. http://dx.doi.org/10.1016/j.febslet.2011.04.042.
10. **Davidson RJ, Davis I, Willey BM, Rizg K, Bolotin S, Porter V, Polsky J, Daneman N, McGeer A, Yang P, Scolnik D, Rowsell R, Imas O, Silverman MS.** 2008. Antimalarial therapy selection for quinolone resistance among *Escherichia coli* in the absence of quinolone exposure, in tropical South America. PLoS One **3:**e2727. http://dx.doi.org/10.1371/journal.pone.0002727.
11. **D'Alessandro S, Corbett Y, Ilboudo DP, Misiano P, Dahiya N, Abay SM, Habluetzel A, Grande R, Gismondo MR, Dechering KJ, Koolen KM, Sauerwein RW, Taramelli D, Basilico N, Parapini S.** 2015. Salinomycin and other ionophores as a new class of antimalarial drugs with transmission-blocking activity. Antimicrob Agents Chemother **59:**5135–5144. http://dx.doi.org/10.1128/AAC.04332-14.
12. **Gumila C, Ancelin ML, Delort AM, Jeminet G, Vial HJ.** 1997. Characterization of the potent *in vitro* and *in vivo* antimalarial activities of ionophore compounds. Antimicrob Agents Chemother **41:**523–529.
13. **Adovelande J, Schrevel J.** 1996. Carboxylic ionophores in malaria chemotherapy: the effects of monensin and nigericin on *Plasmodium falciparum in vitro* and *Plasmodium vinckei petteri in vivo*. Life Sci **59:**PL309-315.
14. **Gumila C, Ancelin ML, Jeminet G, Delort AM, Miquel G, Vial HJ.** 1996. Differential *in vitro* activities of ionophore compounds against *Plasmodium falciparum* and mammalian cells. Antimicrob Agents Chemother **40:**602–608.
15. **Yoon MJ, Kang YJ, Kim IY, Kim EH, Lee JA, Lim JH, Kwon TK, Choi KS.** 2013. Monensin, a polyether ionophore antibiotic, overcomes TRAIL resistance in glioma cells via endoplasmic reticulum stress, DR5 upregulation and c-FLIP downregulation. Carcinogenesis **34:**1918–1928.
16. **Huczyński A.** 2012. Polyether ionophores-promising bioactive molecules for cancer therapy. Bioorg Med Chem Lett **22:**7002–7010.
17. **Griffin T, Rybak ME, Recht L, Singh M, Salimi A, Raso V.** 1993. Potentiation of antitumor immunotoxins by liposomal monensin. J Natl Cancer Inst **85:**292–298. http://dx.doi.org/10.1093/jnci/85.4.292.
18. **Tyagi N, Ghosh PC.** 2011. Folate receptor mediated targeted delivery of ricin entrapped into sterically stabilized liposomes to human epidermoid carcinoma (KB) cells: effect of monensin intercalated into folate-tagged liposomes. Eur J Pharm Sci **43:**343–353.
19. **Simjee S, Heffron AL, Pridmore A, Shryock TR.** 2012. Reversible

monensin adaptation in *Enterococcus faecium*, *Enterococcus faecalis* and *Clostridium perfringens* of cattle origin: potential impact on human food safety. J Antimicrob Chemother **67:**2388–2395. http://dx.doi.org/10.1093/jac/dks236.
20. **Chapman HD, Jeffers TK, Williams RB.** 2010. Forty years of monensin for the control of coccidiosis in poultry. Poult Sci **89:**1788–1801.
21. **Roth JA, Ames RS, Fry K, Lee HM, Scannon PJ.** 1988. Mediation of reduction of spontaneous and experimental pulmonary metastases by ricin A-chain immunotoxin 45-2D9-RTA with potentiation by systemic monensin in mice. Cancer Res **48:**3496–3501.
22. **Schwendener RA, Schott H.** 2010. Liposome formulations of hydrophobic drugs. Methods Mol Biol **605:**129–138. http://dx.doi.org/10.1007/978-1-60327-360-2_8.
23. **Hong SS, Kim SH, Lim SJ.** 2015. Effects of triglycerides on the hydrophobic drug loading capacity of saturated phosphatidylcholine-based liposomes. Int J Pharm **483:**142–150. http://dx.doi.org/10.1016/j.ijpharm.2015.02.013.
24. **Immordino ML, Dosio F, Cattel L.** 2006. Stealth liposomes: review of the basic science, rationale, and clinical applications, existing and potential. Int J Nanomedicine **1:**297–315. http://dx.doi.org/10.2217/17435889.1.3.297.
25. **Torchilin VP.** 2005. Recent advances with liposomes as pharmaceutical carriers. Nat Rev Drug Discov **4:**145–160. http://dx.doi.org/10.1038/nrd1632.
26. **Vasandani VM, Madan S, Ghosh PC.** 1992. *In vivo* potentiation of ricin toxicity by monensin delivered through liposomes. Biochim Biophys Acta **1116:**315–323. http://dx.doi.org/10.1016/0304-4165(92)90046-W.
27. **Tyagi RK, Garg NK, Jadon R, Sahu T, Katare OP, Dalai SK, Awasthi A, Marepally SK.** 2015. Elastic liposome-mediated transdermal immunization enhanced the immunogenicity of *P. falciparum* surface antigen, MSP-119. Vaccine **33:**4630–4638. http://dx.doi.org/10.1016/j.vaccine.2015.06.054.
28. **Alving CR, Schneider I, Swartz GM, Jr, Steck EA.** 1979. Sporozoite-induced malaria: therapeutic effects of glycolipids in liposomes. Science **205:**1142–1144. http://dx.doi.org/10.1126/science.382358.
29. **Peeters PA, Huiskamp CW, Eling WM, Crommelin DJ.** 1989. Chloroquine containing liposomes in the chemotherapy of murine malaria. Parasitology **98**(Pt 3)**:**381–386.
30. **Owais M, Varshney GC, Choudhury A, Chandra S, Gupta CM.** 1995. Chloroquine encapsulated in malaria-infected erythrocyte-specific antibody-bearing liposomes effectively controls chloroquine-resistant *Plasmodium berghei* infections in mice. Antimicrob Agents Chemother **39:**180–184. http://dx.doi.org/10.1128/AAC.39.1.180.
31. **Golab T, Barton SJ, Scroggs RE.** 1973. Colorimetric method for monensin. J Assoc Off Anal Chem **56:**171–173.
32. **Stewart JC.** 1980. Colorimetric determination of phospholipids with ammonium ferrothiocyanate. Anal Biochem **104:**10–14. http://dx.doi.org/10.1016/0003-2697(80)90269-9.
33. **Peter W, Portus H, Robinson L.** 1995. The four day suppressive *in vivo* antimalarial test. Ann Trop Med Parasitol **69:**155–171.
34. **Ma C, Harrison P, Wang L, Coppel RL.** 2010. Automated estimation of parasitaemia of *Plasmodium yoelii*-infected mice by digital image analysis of Giemsa-stained thin blood smears. Malar J **9:**348. http://dx.doi.org/10.1186/1475-2875-9-348.
35. **Gupta R, Rajendran V, Ghosh PC, Srivastava S.** 2014. Assessment of anti-plasmodial activity of non-hemolytic, non-immunogenic, non-toxic antimicrobial peptides (AMPs LR14) produced by *Lactobacillus plantarum* LR/14. Drugs R D **14:**95–103. http://dx.doi.org/10.1007/s40268-014-0043-y.
36. **Hasan GM, Garg N, Dogra E, Surolia R, Ghosh PC.** 2011. Inhibition of the growth of *Plasmodium falciparum* in culture by stearylamine-phosphatidylcholine liposomes. J Parasitol Res **2011:**120462. http://dx.doi.org/10.1155/2011/120462.
37. **Park WH, Lee SJ, Moon HI.** 2008. Antimalarial activity of a new stilbene glycoside from *Parthenocissus tricuspidata* in mice. Antimicrob Agents Chemother **52:**3451–3453. http://dx.doi.org/10.1128/AAC.00562-08.
38. **Sadzuka Y, Kishi K, Hirota S, Sonobe T.** 2003. Effect of polyethyleneglycol (PEG) chain on cell uptake of PEG-modified liposomes. J Liposome Res **13:**157–172. http://dx.doi.org/10.1081/LPR-120020318.
39. **Bhavsar SK, Eberhard M, Bobbala D, Lang F.** 2010. Monensin induced suicidal erythrocyte death. Cell Physiol Biochem **25:**745–752. http://dx.doi.org/10.1159/000315094.
40. **Gumila C, Miquel G, Seta P, Ancelin ML, Delort AM, Jeminet G, Vial HJ.** 1999. Ionophore-phospholipid interactions in Langmuir films in relation to ionophore selectivity toward *Plasmodium*-infected erythrocytes. J Colloid Interface Sci **218:**377–387. http://dx.doi.org/10.1006/jcis.1999.6432.
41. **Yoshihara E, Nakae T.** 1986. Cytolytic activity of liposomes containing stearylamine. Biochim Biophys Acta **854:**93–101. http://dx.doi.org/10.1016/0005-2736(86)90068-4.
42. **Tokumasu F, Ostera GR, Amaratunga C, Fairhurst RM.** 2012. Modifications in erythrocyte membrane zeta potential by *Plasmodium falciparum* infection. Exp Parasitol **131:**245–251. http://dx.doi.org/10.1016/j.exppara.2012.03.005.
43. **Eda S, Sherman IW.** 2002. Cytoadherence of malaria-infected red blood cells involves exposure of phosphatidylserine. Cell Physiol Biochem **12:**373–384. http://dx.doi.org/10.1159/000067908.
44. **Borowik T, Widerak K, Ugorski M, Langner M.** 2005. Combined effect of surface electrostatic charge and poly(ethyl glycol) on the association of liposomes with colon carcinoma cells. J Liposome Res **15:**199–213. http://dx.doi.org/10.1080/08982100500364370.
45. **Romberg B, Oussoren C, Snel CJ, Hennink WE, Storm G.** 2007. Effect of liposome characteristics and dose on the pharmacokinetics of liposomes coated with poly(amino acid)s. Pharm Res **24:**2394–2401. http://dx.doi.org/10.1007/s11095-007-9393-2.
46. **Zalipsky S, Brandeis E, Newman MS, Woodle MC.** 1994. Long-circulating, cationic liposomes containing amino-PEG-phosphatidylethanolamine. FEBS Lett **353:**71–74. http://dx.doi.org/10.1016/0014-5793(94)01013-7.
47. **Levchenko TS, Rammohan R, Lukyanov AN, Whiteman KR, Torchilin VP.** 2002. Liposome clearance in mice: the effect of a separate and combined presence of surface charge and polymer coating. Int J Pharm **240:**95–102. http://dx.doi.org/10.1016/S0378-5173(02)00129-1.
48. **Dos Santos N, Allen C, Doppen AM, Anantha M, Cox KA, Gallagher RC, Karlsson G, Edwards K, Kenner G, Samuels L, Webb MS, Bally MB.** 2007. Influence of poly(ethylene glycol) grafting density and polymer length on liposomes: relating plasma circulation lifetimes to protein binding. Biochim Biophys Acta **1768:**1367–1377. http://dx.doi.org/10.1016/j.bbamem.2006.12.013.
49. **Nakornchai S, Sathitudsahakorn C, Chongchirasiri S, Yuthavong Y.** 1983. Mechanism of enhanced fusion capacity of mouse red cells infected with *Plasmodium berghei*. J Cell Sci **63:**147–154.
50. **Pozzi D, Colapicchioni V, Caracciolo G, Piovesana S, Capriotti AL, Palchetti S, De Grossi S, Riccioli A, Amenitsch H, Lagana A.** 2014. Effect of polyethyleneglycol (PEG) chain length on the bio-nano-interactions between PEGylated lipid nanoparticles and biological fluids: from nanostructure to uptake in cancer cells. Nanoscale **6:**2782–2792. http://dx.doi.org/10.1039/c3nr05559k.
51. **Postma NS, Crommelin DJ, Eling WM, Zuidema J.** 1999. Treatment with liposome-bound recombinant human tumor necrosis factor-alpha suppresses parasitemia and protects against *Plasmodium berghei* k173-induced experimental cerebral malaria in mice. J Pharmacol Exp Ther **288:**114–120.
52. **Lambros C, Vanderberg JP.** 1979. Synchronization of *Plasmodium falciparum* erythrocytic stages in culture. J Parasitol **65:**418–420.